Iranian Polymer Journal
16 (11), 2007, 731-739

Available online at: http://journal.ippi.ac.ir

Velocity Distribution of Helical Ribbon Impeller in Mixing of Polymeric Liquids in the Transition Region

Mansour Jahangiri

Chemical Engineering group, University of Semnan, Semnan, Iran

Received 19 April 2006; accepted 20 October 2007

A B S T R A C T

Velocity profiles are helpful for the confident design of mixing tanks in the transition region. In this article, velocity profiles for helical ribbon impeller have been studied using laser Doppler anemometry for viscoelastic liquids with rheological properties typical of those found in polymer processes. Local tangential and radial velocities were measured at radial positions on a horizontal plane passing through the middle of the helical ribbon impeller. New correlation is suggested for dimensionless local tangential velocity profiles in the transition region, i.e. $70<N_{Re}<6700$. Experimental results show that the magnitudes of dimensionless radial velocities are much less than dimensionless mean tangential velocities such that no considerable radial flow could be detected.

Key Words:

LDA;
helical ribbon impeller;
viscoelastic liquids;
mixing.

INTRODUCTION

Stirred tank reactors are important components of the processing plants in many branches of industry such as polymeric processes and chemical industry [1]. Considerable research efforts have been devoted to mixing in agitated vessels focus on classical impellers such as propellers and turbines [2]. These impellers are known to have low efficiency when mixing non-Newtonian fluids particularly those with elastic properties [3]. In mixing of non-Newtonian liquids, helical ribbon impellers operate slowly and do not create high velocity gradients. They rely on an excellent pumping capacity that reaches

(*) To whom correspondence to be addressed.
E-mail: M_Jahan98@yahoo.com

every corner of the vessel [4]. Helical ribbon impellers are capable of producing vertical circulation patterns (axial pumping) over the entire vessel volume and they have a fairly good homogenization potential for mixing of viscous Newtonian and non–Newtonian liquids [5]. Most of previous works are limited to the laminar flow region [6-8]. Only a few works on the mixing of viscoelastic liquids with helical ribbon impellers in the transition region are available in the literature [9-11]. Investigation of the detailed velocity profiles can provide the most useful information for analyzing the performance of the impeller [12,13]. The influence of viscoelasticity on the flow pattern is complex [3]. Carreau et al. [14] in the mixing of viscoelastic fluids with helical ribbon agitators showed that the velocity profiles were qualitatively similar for all the fluids. However, they also found a decreasing axial circulation and an increasing circumferential flow as fluid elasticity increased.

Laser Doppler Anemometry (LDA) has proven to be more accurate in the measurement of flow fields in stirred tanks than any other methods such as Pitot probes and hot–wire anemometers because: (a) it provides flow information even in unsteady and highly turbulent flow regions as well as in the return flow areas of the tank, and (b) it operates without fluid contact [15]. Though LDA is being increasingly applied to stirred vessels, no LDA velocity measurements have been reported about viscoelastic fluids with helical ribbon impellers [16,17]. Most studies are concerned with LDA velocity measurements of Rushton turbines for Newtonian and non–Newtonian fluids [18-21]. In this paper, the variations of local velocity components on a horizontal plane passing nearly through the middle height of the helical ribbon impeller via LDA are measured. Efforts have been made to establish a relationship between the helical ribbon impeller velocity and the elasticity of polyacrylamide (PAA) solutions through dimensionless groups such as the elasticity and Weissenberg numbers.

EXPERIMENTAL

Mixing experiments were performed in a cylindrical Plexiglas tank with an inside diameter of D = 276 mm and a wall thickness of 3 mm. The height of the liquid in the tank was kept at 210 mm. The impeller was a single helical ribbon with 40º pitched blade, diameter of d = 255 mm and thickness of 1.0 mm. The geometrical ratios of D/d, w/d, p/d, h/d of the typical helical

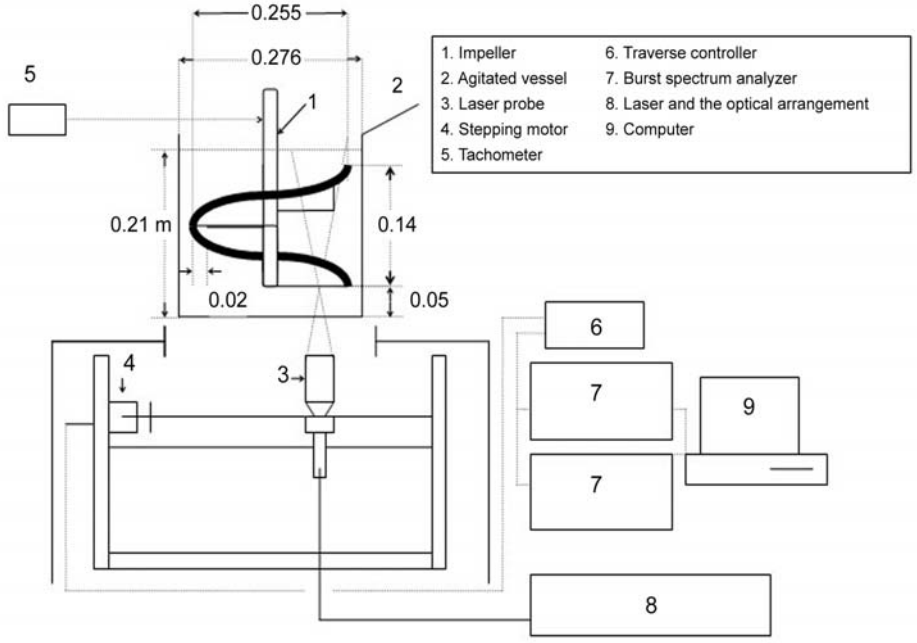

Figure 1. Setup of LDA and agitated vessel for mixing of viscoelastic liquids (all dimensions are in meter).

ribbon impeller reported in this article are respectively, 1.0824, 0.549, 0.549, 0.1176 nearly similar to ref. [3,8]. Where D, w, p and h were tank diameter, impeller blade width, pitch and height of impeller, respectively. The tank and the helical ribbon configurations are shown in Figure 1. The impeller was driven by a variable speed motor. A laser probe was used to measure the radial and tangential components of the fluid velocity. To obtain a uniform refraction of the laser beams, the probe was mounted on a motor-controlled traversing mechanism allowing the experimenter to conduct a complete scan of the mixing tank from underneath. The system consisted of a 5 W Spectra-Physics argon-ion laser, two-colour modular optics, two burst spectrum analyzers and a PC. The front focusing lens had a focal length of 310 mm and produced a beam angle of 9.92º. The power of the emitted blue-green beam could be regulated up to 5 W. This beam was split by a modular optical system into four beams in such a way that two of them were blue rays having a wavelength of 488.0 nm and two others were green with a wavelength of 514.5 nm. Radial and tangential velocities could be obtained simultaneously when the probe traversed along the radius of the mixing vessel. Tangential velocities were obtained using green beams and radial velocities via blues. The LDA system (Dantec Measurement Technology) was operated in the backscatter mode with both receiving and transmitting optics in the same module. The natural ingredients of the polyacrylamide solution of this work were suitable for LDA because for 20k bursts, the data rates up to over 1 kHz were easily obtained with over 60% validity and therefore no seeding was required [22]. The total number of the collected bursts at each point was such that for any larger number of bursts, only the variations less than 10 mm/s in the velocity could be sensed. An oversize filter accepted only the signals from the smallest particles. Calculated average values could be biased in such flows. The continuous-wave mode of measurement took more data from slower-moving particles and in this way reduced the bias error to less than two percent [23].

Polyacrylamide LT27 from Magnofloc UK was dissolved in 50 wt% glycerine-water mixtures at four concentrations of 500, 900, 1100 and 1350 ppm. The fluids were denoted as A, B, C and D, respectively. Steady state and oscillatory shear experiments were performed with a computer-controlled rheometer RV100/CV100 from Haake. The viscometric data were obtained at 15ºC being the same temperature as that encountered in the mixing experiments.

RHEOLOGICAL PARAMETERS AND DIMENSIONLESS NUMBERS

The rheological parameters for these fluids were obtained by fitting the steady viscosity $\eta(\dot{\gamma})$ and dynamic viscosity $\eta'(\omega)$ functions to the experimental data. The upper convected Maxwell (UCM) model was modified to provide a satisfactory fit to the data through accommodating the shear-dependent properties of the fluid in the parameters of the model as following [24,25]:

$$\tau + \lambda(II_d)\tau_{(1)} = -2\eta(II_d)d \quad (1a)$$

in which

$$\eta(II_d) = \eta_0/(1 + aII_d^b) \quad (1b)$$

$$\lambda(II_d) = \lambda_0/(1 + cII_d^d) \quad (1c)$$

where II_d is the second invariant of the rate of stretch tensor d. The resulting material functions for steady and oscillatory shear flows have the following forms, respectively.

$$\eta(\dot{\gamma}) = \eta_0/(1 + aII_d^b) \quad (1d)$$

$$\eta'(\omega) = \eta_0/(1 + cII_d^d)^2/[(1 + cII_d^d)^2 + \lambda_0^2\omega^2] \quad (1e)$$

where $\dot{\gamma}$ and ω denote the shear rate and angular frequency of steady and oscillatory shear conditions, respectively; II_d equals to corresponding $\dot{\gamma}^2/4$ and $\omega^2/4$. η_0 and λ_0 denote the zero-shear-rate viscosity and the maximum relaxation time of the fluid. The model parameters a, b, c, and d are obtained by fitting the experimental data.

It has been shown that the key dimensionless group for the reversal flow pattern in the mixing of viscoelastic fluids is the elasticity number defined as follows [26]:

$$El = \frac{Wi}{N_{Re}} \quad (2a)$$

where the Weissenberg and Reynolds numbers are defined as:

$$Wi = \lambda_0 \dot{\gamma}_{tip} \quad (2b)$$

$$N_{Re} = \frac{\rho N D^2}{\eta_0} \quad (2c)$$

in which ρ, D, and $\dot{\gamma}_{tip}$ denote the fluid density, the impeller diameter and the shear rate at the impeller tip which is calculated from Metzner-Otto Method [27,28]:

$$\dot{\gamma}_{tip} = k_s.N \quad (2d)$$

where N is the rotational speed of the impeller in round per second (round/s) and k_s is the Metzner-Otto coefficient.

RESULTS AND DISCUSSION

The steady viscosity data versus shear rate were remarkably similar to those of the dynamic viscosity versus angular frequency supporting the following experimental relationship for polymer solutions:

$$\eta(\dot{\gamma})\big|_{\dot{\gamma}\to 0} = \eta'(\omega)\big|_{\omega\to 0} \quad (3)$$

On the other hand, η_0 and λ_0 can be obtained through the fitting of the dynamic viscosity data alone. Therefore, only the dynamic viscosity data are presented in Figure 2. The solid lines in the figure are the results of the fitting model and the parameters are given in Table 1.

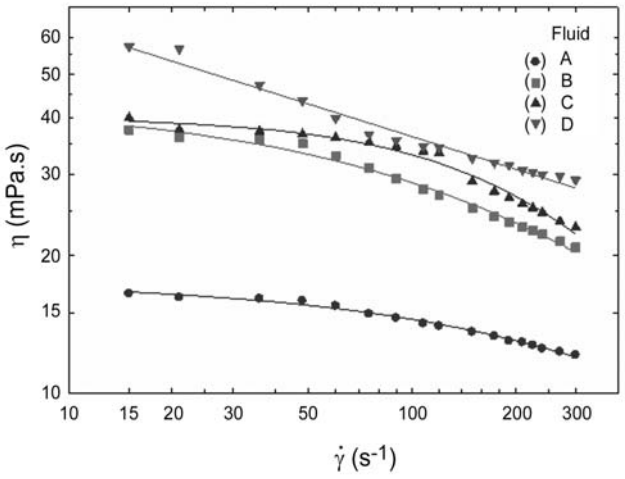

Figure 2. Dynamic viscosity data of PAA solutions. Solid lines are the predictions of the modified-upper-convected Maxwell model.

In order to measure the mean average velocity components in the mixing of the PAA solutions with a helical ribbon impeller, twenty-five radial positions between the impeller shaft and the vessel wall were chosen on the horizontal plane of z/H = 0.57 where z and H denote the vertical coordinate from the bottom of the tank and the height of the tank, respectively. The points were equally spaced such that r_i in mm equaled 10 + 5(i - 1) for i = 1, 2, ..., 25. The origin of the coordinate system used, was the centre of the vessel base plate. The local mean velocities at these points were measured at impeller rotational speeds corresponding to the transition region $70<N_{Re}<6700$.

Tangential Velocity

The velocity histogram of Figure 3a, showing one peak, is typical of the measurements corresponding to radial positions between the impeller shaft and the vicinity of the impeller blade. This region was not

Table 1. Modified upper convected Maxwell model parameters for different PAA solutions.

Fluid	PAA (ppm)	ρ (kg/m^3)	η_0 (mPa.s)	a	b	c	d	λ_0 (s)
A	500	1102.4	17.7	0.039	0.244	0.08	0.58	0.04
B	900	1104.0	41.3	0.079	0.277	0.70	0.45	0.15
C	1100	1104.8	310	0.456	0.323	1.95	0.43	1.20
D	1350	1113.6	420	0.534	0.312	1.75	0.44	1.22

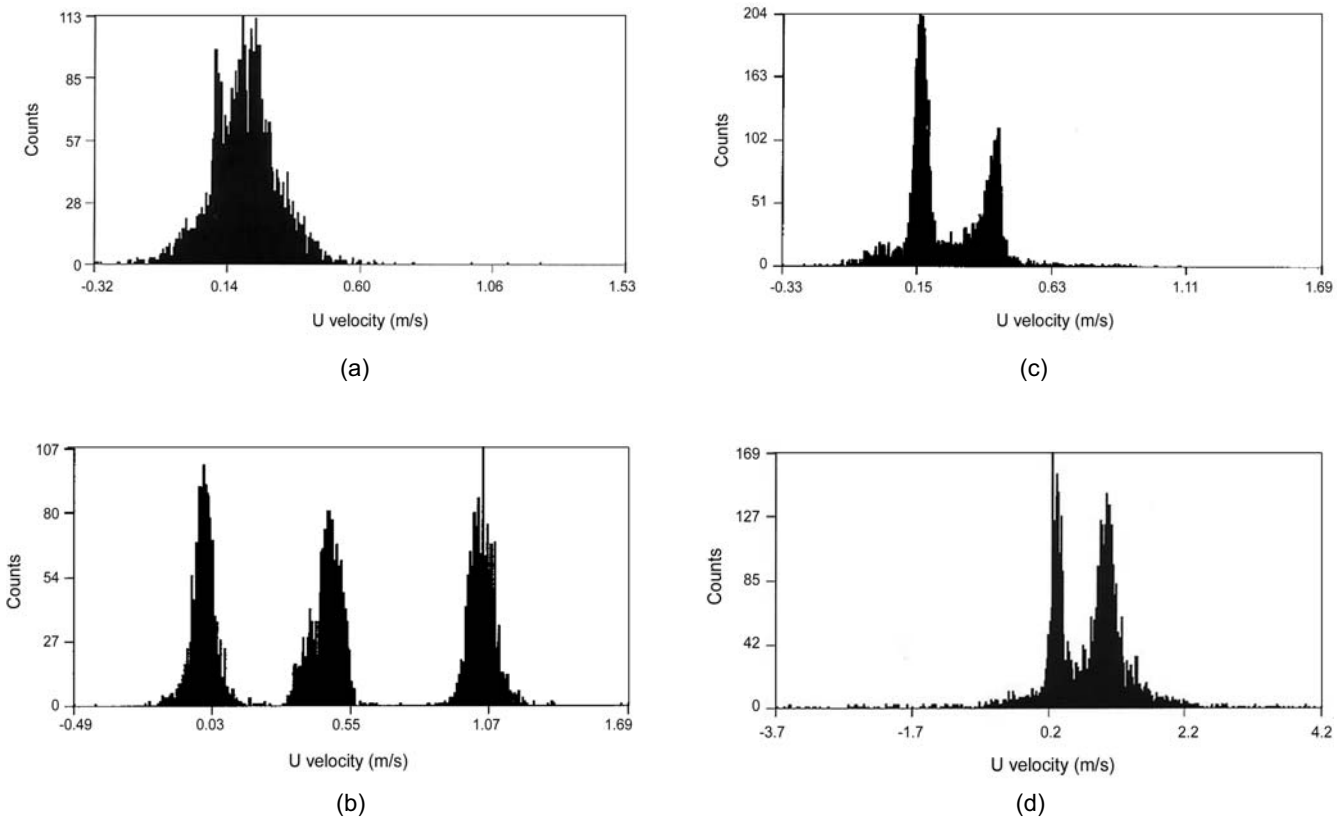

Figure 3. Tangential velocity histograms of: (a) fluid A, (b) fluid C, (c) fluid B, (d) fluid D ((Table 1) with helical ribbon impeller).

swept by the impeller blade. For the region that was swept by the impeller, however, three peaks were obtained at each radial position. A typical example is illustrated in Figure 3b. At smaller rotational speeds (Figure 3c) and/or higher concentrations of PAA solution (Figure 3d), two peaks were observed instead of three because of more significant viscoelastic effects and larger viscosities. Velocity histograms of the tangential component of the velocity were Gaussian anywhere away from the blades. The three peaks meant that the blade passage caused three dominant velocities at each location. In Figures 3a, 3b, 3c and 3d, dominant velocity of each histogram is an average velocity of 5000 liquid particles in each histogram in any given radial position. Thus, an average velocity of 5000 liquid particles is a yield of local velocity in any given radial position. Using eqn (4), average velocity of a velocity histogram or average velocity of 5000 liquid particles in each velocity histogram as a local velocity is calculated knowing velocity of a liquid particle ($v_{\theta i}$) and the number of particles (n_i) available in that velocity histogram. The average velocity for each peak in Figure 3 was calculated through the following equation in which $v_{\theta i}$ and v_θ were the individual and the average tangential velocity of the i^{th} particle and n_i was the number of the particles having the velocity $v_{\theta i}$:

$$v_\theta = \frac{\sum_i v_{\theta i} n_i}{\sum_i n_i} \quad (4)$$

Thus, one, two or three values for the velocities could be obtained at each radial position depending on the particular region in which the observations were made. Figure 4 shows an example of the local tangential velocities at various radial positions obtained through LDA measurements. These velocities are normalized by the blade tip speed, v_{tip}. The results show that the dimensionless tangential velocity distributions for PAA solutions are nearly independent of the impeller rotational speed. This result can be of important design implications with regard to the scale-up rules and it is in agreement with the literature as well

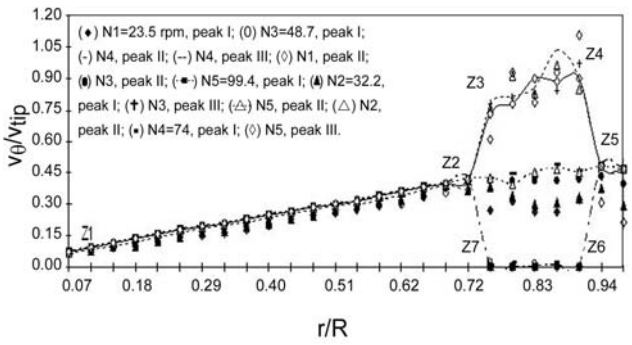

Figure 4. Three zone velocity profiles of helical ribbon impeller for 900 ppm PAA solution at different impeller speeds (the peaks I, II and III are the same as that of Figure 3).

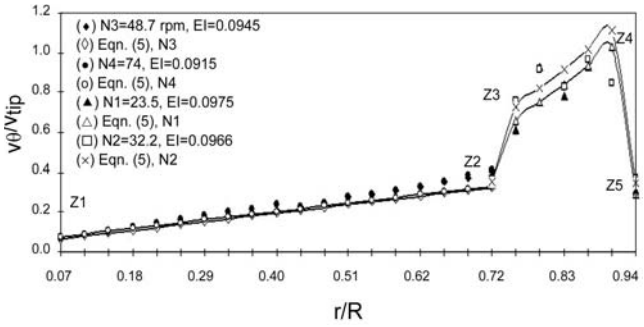

Figure 5. Predicted values of eqn (5) for tangential velocity of helical ribbon impeller in mixing of PAA solutions.

[9,14]. On the other hand, in the space between the shaft and the impeller, the fluid has a rigid body rotation. This zone is referred to as Z1-Z2 in the velocity field versus radius of Figure 4. The value of the dimensionless mean tangential velocity, v_θ/v_{tip}, begins nearly from 0.1 at the radial position r/R = 0.072 and increases to the value of about 0.45 at r/R = 0.7. The steep increase and then reduction in the profiles of v_θ/v_{tip} for the helical ribbon impeller at various impeller speeds occur in the range of r/R > 0.7. The value of v_θ/v_{tip} at the inclined blade surface 0.72< r/R < 0.92 increases slightly with the impeller speed. In Figure 4, the zone referred to as Z3-Z4 corresponds to the third peak (the largest velocity) in Figure 3b and the zone Z7-Z6 to the first peak (the smallest velocity) in Figure 3b. These zones are related to the front and back face of the impeller blade, respectively. Therefore, three velocity gradients along Z2-Z3, Z3-Z4 and Z4-Z5 can exist for each part of the impeller with respect to the bulk fluid velocity along Z2-Z5. There are also two velocity gradients relating to the impeller edges along Z3-Z7 and Z4-Z6. The behaviour of flow wake in the latter zones is not definitely established in this work and further investigation seems necessary. Thus, the front face of impeller blade is considered in this work for the calculation of the shear rate due to its large velocity gradients with respect to the bulk fluid.

To find suitable correlations for the profiles of v_θ/v_{tip} at the front face of the impeller blade in the transition region, several relationships were examined following the works of Cheng et al. [11] and Carreau et al. [14]. It was concluded that these velocity profiles could be obtained satisfactorily through the consideration of two zones instead of one. The first zone relied between the impeller shaft and the impeller blade Z1-Z2. The second one was related to the neighbourhood of the impeller blade at the front face Z2-Z3-Z4-Z5. The following equation fairly correlated the mean tangential velocity with the impeller speed for PAA solutions in the transition region of 70 < N_{Re}< 6700.

$$v_\theta / v_{tip} = m_0 + n_0 (r/R) \quad (5)$$

where m_0 and n_0 are given in Table 2 for various zones of Figure 5. In this equation, the ranges of N_{Re} and El are 70 <N_{Re}< 6700 and 0.07 <El< 0.11, respectively. Error analysis using standard deviation (SD)

Table 2. Coefficients of the velocity profile of eqn (5).

Zone	m_0	n_0
Z1–Z2	0.000002 N_{Re} + 0.999949El	0.000108 N_{Re} + 0.999905El
Z2–Z3	0.000397 N_{Re} + 1.009603El	1.001172 N_{Re} + 1.00827El
Z3–Z4	0.00005 N_{Re} + 1.00995El	0.001169 N_{Re} + 1.00883El
Z4–Z5	-0.000379 N_{Re} + 1.0710379El	0.001174 N_{Re} + 1.08825El

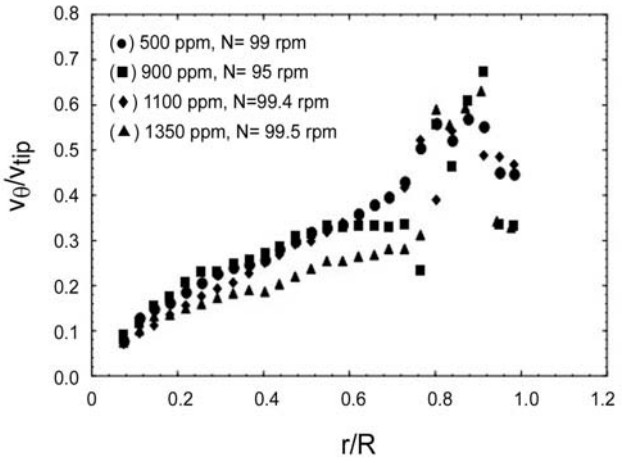

Figure 6. Dimensionless tangential velocities for different concentrations of PAA solutions.

and local relative error (ε) shows that the mean deviations between the correlation results of eqn (5) and the experimental data are given in Table 2 for PAA solutions of this work at different impeller speeds is about 11.5% [29]. The results lead to the conclusion that linear correlations such as those given here are suitable relationships for correlating v_θ/v_{tip} data in the transition region.

The effect of PAA concentration on the velocity profile nearly at the same value of impeller speed is given in Figure 6. This figure shows the decrease in the tangential velocity component at all radial positions with increasing the PAA concentration.

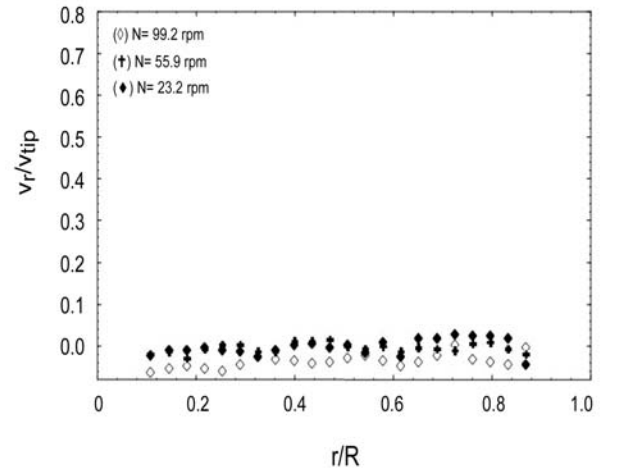

Figure 7. Dimensionless radial velocities of helical ribbon impeller versus radial for 1350 ppm PAA solution and different impellers.

Radial Velocity

Figure 7 demonstrates an example of the dimensionless radial velocity, v_r/v_{tip}, for 1350 ppm PAA solution at various impeller speeds corresponding to the Reynolds number in the transition region. The radial velocities of the PAA solutions are much less than their tangential counterparts. Indeed, the results reveal that no considerable radial velocities could be measured. These results are in agreement with the findings of Cheng et al. [11] and Carreau et al. [14] and are different from those of Shekhar et al. [21].

CONCLUSION

LDA velocity measurements in different concentrations of polyacrylamide (PAA) solutions for a helical ribbon impeller have produced results in the transition region, i.e. $70 < N_{Re} < 6700$ as follows:

1. Prevailing flow patterns in the mixing of PAA solutions are tangential and no considerable radial velocity could be obtained.
2. The dimensionless local tangential velocity distributions were reasonably correlated considering two regions using linear relationships.
3. The dimensionless local tangential velocity profiles versus dimensionless radial coordinate nearly were not affected by impeller rotational speed.

SYMBOLS AND ABBREVIATIONS

a,b,c,d constants in modified upper convected Maxwell model
D impeller diameter (m)
H height of liquid in agitated vessel
d stretch tensor, $d = 1/2\ (\nabla v+(\nabla v)^{\dagger})$
El elasticity number
k_s Metzner-Otto coefficient
M shear rate factor
N rotational speed (round/s)
r radial coordinate (m)
R radius of agitated vessel (m)
N_{Re} Reynolds number
SD standard deviation
T agitated vessel diameter (m)
∇v velocity gradient

v_r radial velocity (m/s)
v_θ tangential velocity (m/s)
v_{tip} impeller blade tip speed (m/s)
z axial coordinate (m)
Wi Weissenberg number

GREEK SYMBOLS

ε_i local relative error, $(f_{i,exp}-f_{i,pred})/f_{i,exp}$
$\dot{\gamma}_{tip}$ impeller tip shear rate (s^{-1})
η_0 zero shear rate viscosity (Pa.s)
$\eta(\dot{\gamma})$ steady state viscosity (Pa.s)
$\eta'(\omega)$ dynamic viscosity (Pa.s)
λ_0 zero shear rate Maxwell relaxation time (s)
ρ fluid density (kg/m^3)
τ stress tensor (Pa)
ω angular frequency of oscillatory shear flow (rad/s)
II_d second invariant of the stretch tensor, $II_d = 1/2\ (d:d^{\dagger})$

SUPERSCRIPT

$\dagger$ transpose of a second order tensor

SUBSCRIPTS

(1) first upper convected time derivative
pred predicted values proposed by correlations
exp experimental data
r, θ radial and tangential components, respectively.

REFERENCES

1. Smith J.M., Industrial needs for mixing research, *Trans. Inst. Chem. Eng.*, **68**, 3-6, 1990.
2. Escudie R., Bouyer D., Line A., Characterization of trailing vortices generated by a Rushton turbine, *AIChE J.*, **50**, 75-86, 2004.
3. Ulbrecht J., Carreau P.J., Mixing of Viscous Non-Newtonian Liquids, In: *Mixing of Liquids by Mechanical Agitation*, Ulbrecht J.J., Patterson G.K. (Eds.), Gordon and Breach, New York, 1985.
4. Brito-De La Fuente E., Leuliet J.C., Choplin L., Tanguy P.A., On the effect of shear thinning behavior on mixing with helical ribbon impeller, *Chem. Eng. Res. Des.*, **69**, 324, 1991.
5. Yap C.Y., Patterson W.I., Carreau P.J., Mixing with helical ribbon agitators, *AIChE J.*, **25**, 516-521, 1979.
6. Tatterson G.B., *Fluid Mixing and Gas Dispersion in Agitated Tanks*, McGraw-Hill, New York, 1991.
7. De La Villeon J., Bertrand F., Tanguy P.A., Labrie R., Bousquet J., Lebouvier D., Numerical investigation of mixing efficiency of helical ribbons, *AIChE J.*, **44**, 972-977, 1998.
8. Carreau P.J., Chhabra R.P., Cheng J., Effect of rheological properties on power consumption with helical ribbon agitators, *AIChE J.*, **39**, 1421-1430, 1993.
9. Jahangiri M., Golkar-Narenji M.R., Montazerin N., Savarmand S., Shear rate and velocity profiles of a helical ribbon impeller in the transition region through LDA studies, *Proc. Polym. Proc. Soc. Conf.*, Zlin, 219-220, Czech Rep., August 16-18, 2000.
10. Bertrand F.B., Tanguy P.A., Brito de la Fuente E., Carreau P.J., Numerical modeling of the mixing flow of second order fluids with helical ribbon impellers, *Comput. Methods Appl. Mech. Eng.*, **180**, 267-280, 1999.
11. Cheng J., Carreau P.J., Mixing in the transition flow regime with helical ribbon agitators, *Can. J. Chem. Eng.*, **72**, 418-430, 1994.
12. Jahangiri M., An LDA study of the Rushton turbine velocity profile for mixing of polymeric liquids, *Iran. Polym. J.*, **14**, 521-530, 2005.
13. Jahangiri M., Fluctuation velocity for non-Newtonian liquids in mixing tank by Rushton turbine in the transition region, *Iran. Polym. J.*, **15**, 285-290, 2006.
14. Carreau P.J., Patterson I., Yap C.Y., Mixing of viscoelastic fluids with helical-ribbon agitators. I. Mixing time and flow patterns, *Can. J. Chem. Eng.*, **54**, 135-142, 1976.
15. Li M., White G., Wilkinson D., Roberts K.J., LDA Measurements and CFD modeling of a stirred vessel with a retreat curve impeller, *Ind. Eng. Chem. Res.*, **43**, 6534-6547, 2004.
16. Van der Molen K., Van Maanen H.R.E., Laser-

doppler measurements of the turbulent flow in stirred vessels to establish scaling rules, *Chem. Eng. Sci.*, **33**, 1161-1168, 1978.
17. Nouri J.M., Whitelaw J.H., Flow characteristics of stirred reactors with Newtonian and non-Newtonian fluids, *AIChE J.*, **36**, 627-629, 1990.
18. Wu H., Patterson G.K., Laser-doppler measurements of turbulent flow parameters in a stirred mixer, *Chem. Eng. Sci.*, **44**, 2207-2221, 1989.
19. Koutsakos E., Nienow A.W., Dyster K.N., Laser anemometry study of shear thinning fluids agitated by a Rushton turbine, Fluid Mixing IV, Bradford, UK, *IChemE Symp. Ser. No.*, **121**, 51-73, 1990.
20. Dyster K.N., Koutsakos E., Jaworski Z., Nienow A.W., An LDA study of the radial discharge velocities generated by a Rushton turbine: Newtonian fluids, Re ≥ 5, *Trans. IChemE, Eng. Res. Des.*, **71**, 11-23, 1993.
21. Shekhar S.M., Jayanti S., Mixing of pseudoplastic fluids using helical ribbon impellers, *AIChE J.*, **49**, 2768-2772, 2003.
22. Montazerin N., Damangir A., Mirian S., A new concept for squirrel-cage fan inlet, *Proc. Instn. Mech. Eng. Part A: J. Power Energy*, **212**, 343-349, 1998.
23. Johnson D.A., Modarress D., Owen F.K., An experimental verification of laser velocimeter sampling bias and its correlation, *Trans. ASME J. Fluids Eng.*, **106**, 5-12, 1984.
24. Savarmand S., Narenji M.R.G., Wilkinson W.L., Modifications to non-linear rheological models of viscoelastic fluids, *Iran. Polym. J.*, **7**, 195-203, 1998.
25. Golkar-Narenji M.R., *Free Coating of Viscoelastic Fluids*, PhD Thesis, University of Bradford, UK, 1, 79, 1978.
26. Ulbrecht J., Mixing of viscoelastic fluids by mechanical agitation, *Chem. Eng.*, **286**, 347-353, 367, 1974.
27. Jahangiri M., Golkar-Narenji M.R., Montazerin N., Savarmand S., Investigation of the viscoelastic effect on the Metzner and Otto coefficient through LDA velocity measurements, *Chin. J. Chem. Eng.*, **9**, 77-83, 2001.
28. Doraiswamy D., Grenville R.K., Etchells A.W., Two-score years of the Metzner-Otto correlation, *Ind. Eng. Chem. Res.*, **33**, 2253-2258, 1994.
29. Walpole R.E., Myers R.H., Myers S.L., *Probability and Statistics for Engineers and Scientists*, Printice Hall Int. l, 6/E, 92-100, 586-594, 1998.